doi:10.1038/nature11823

Figure S1. Retinal angiogenesis is regulated by light

Retinal angiogenesis in mice begins at the day of birth with the extension of vessel precursors from the head of the optic nerve. A superficial layer of vasculature within the retinal ganglion cell (RGC) layer has extended to the retinal periphery by P7. Starting at about P8, angiogenic sprouts extend vertically downwards into the deeper layers of the retina. These sprouts turn and branch and ultimately form the deep vasculature at the outer edge of the inner nuclear layer and the intermediate plexus within the inner plexiform layer[1]. Thus, in control P8 retina, the superficial vascular layer has extended to the periphery (Fig. S1a). At this stage, a section of vasculature half way to the periphery has the appearance of a fine network (Fig. S1b). Adjacent to veins, a normal P8 vasculature shows vessels of slightly higher density and caliber (Fig. S1c). As revealed by depth color-coding of a confocal image stack, at P8, a few angiogenic sprouts (Fig. S1d, yellow) have started to descend vertically through the retina from the superficial layer (Fig. S1d, orange) to the deeper layers. Retinal myeloid cells that label faintly with isolectin and are positioned between vessels, are observed in the deep layer vasculature[1] (Fig. S1d, blue).

In mice dark-reared from E16-17, the superficial vascular plexus (Fig. S1e) showed an increase in density regardless of whether the region was simple plexus (Fig. S1f) or at a vein (Fig. S1g). Depth-coded P8 image stacks (Fig. S1h) showed that there were many more descending vessels (Fig. S1h, yellow, blue) than in the wild type (Fig. S1d, yellow) and many of these were abnormally located. Quantification revealed a significant increase in the number of branch-points in the superficial vasculature of dark-reared mice (Fig. Fig. S1i) and a significant increase in the number of vertical sprouts (Fig. S1j). Thus, the retinal vasculature is a second vascular structure in the eye where normal development is disrupted by the absence of light.

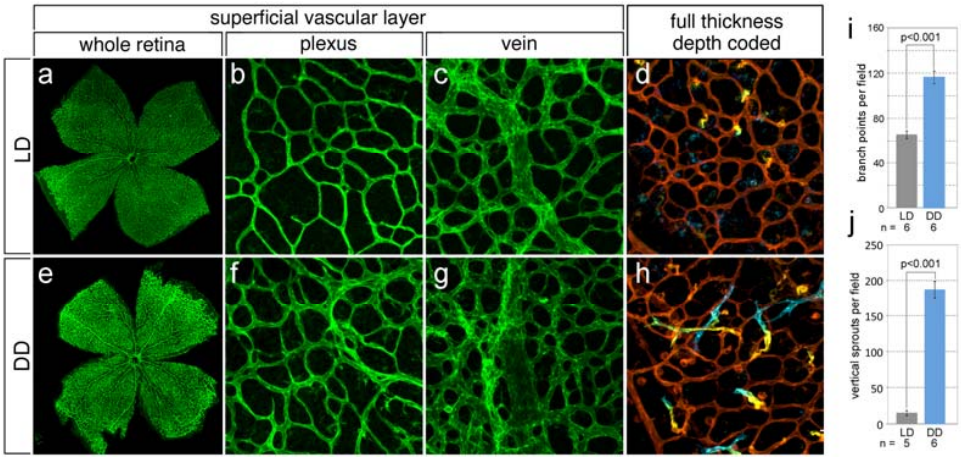

Figure S1 | Retinal vascular phenotypes in dark reared animals. Low (a, e) and high (b, c, d, f, g, h) magnification images of isolectin-labeled P8 retinae from (a-d) wild type pups raised under normal lighting (LD), and (e-h) dark-reared (DD) pups. (e, j) Depth-coded z stack images for each condition indicate the appearance of vertical angiogenic sprouts. Orange represents the superficial vascular layer, blue the deep vascular layer and yellow/green, the intermediate. In (j) the deeper vascular plexus is already forming as indicated by blue color and there are many yellow color vessels suggesting that angiogenic sprouts are descending precociously. Graphs (i, j) shows quantification of superficial plexus branch points and descending sprouts in LD and DD animals. Errors bars are SEM. Sample size indicated below the charts. p value obtained using Student's T-test.

Figure S2. Hyaloid vessel regression is regulated by the *Opn4* gene product melanopsin

Melanopsin is expressed from an early stage of both mouse and human gestation and unlike photoreceptor opsins, is known to function in the mouse eye before P10[2]. Melanopsin expressing ipRGCs (intrinsically photosensitive retinal ganglion cells)[3,4] are a subset of RGCs that can be visualized in the E15 (Fig. S2a) and P5 retina (Fig. S2b, c). When cre recombinase is targeted to the melanopsin gene *Opn4*[5] and used to convert the *Ai4* reporter, red fluorescent, immature ipRGCs are apparent at E15 (Fig. 2a). Double labeling for vasculature (Fig. S2b, green) and melanopsin (Fig. S2b, c, red) shows that at P5, ipRGCs are found in the superficial layers of the retina immediately adjacent to forming retinal vasculature and juxtaposed to the hyaloid vessels in the vitreous. This location made melanopsin a good candidate to mediate light-dependent vascular development in the eye.

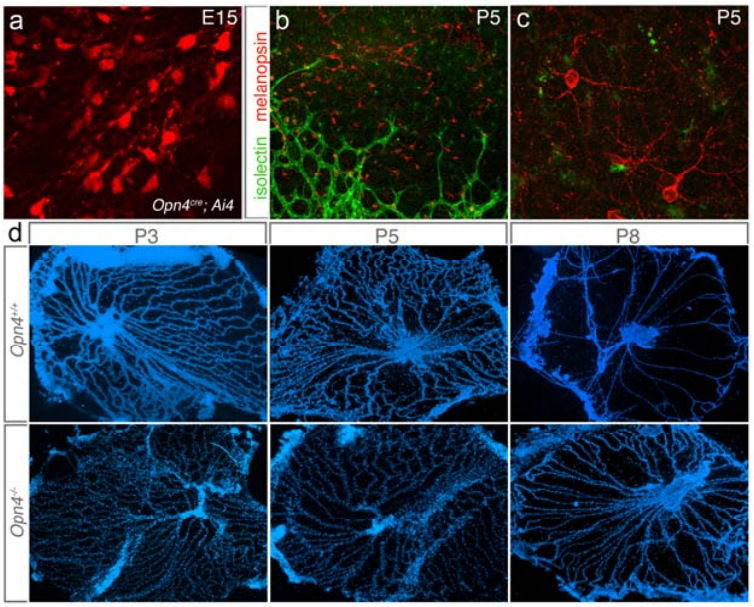

Figure S2 | Hyaloid vessels persists at P8 in the *Opn4*$^{-/-}$ mice. (a) Detection of melanopsin expressing ipRGCs (red) at E15 in retinal whole mounts from *Opn4*$^{Cre/+}$; *Ai4* animals. (b-c) retinal vasculature (green, isolectin labeling) and melanopsin in ipRGCs (red) in the superficial layers of the P5 mouse retina. (b) Is at 100x magnification and is located at the extending front of retinal vessels. (b) Is at 400x magnification of position peripheral to the extending vascular front. Retinal myeloid cells in (b, c) can be observed labeled at low levels with isolectin (green). (d) Hyaloid vessel preparations at P3, P5 and P8 for control and *Opn4*$^{-/-}$ mice. (e) *Opn4*$^{-/-}$ mice over a P1 to P8 time- course.

To test this possibility, we assessed both hyaloid vessel regression and retinal vascular development in mice mutated in *Opn4,* the melanopsin-encoding gene[6,7]. *Opn4*$^{-/-}$ mice showed normal hyaloid vessel numbers at P1 (Fig. S2d, Fig. 2a) but a robust persistence at P8 (Fig. S2d, Fig. 2a). Examination of P15 eyes showed hyaloid regression was complete in the *Opn4*$^{-/-}$ mice indicating that, as with dark-reared mice, though hyaloid regression was significantly delayed, persistence was not long-term.

Figure S3. Retinal vascular defects persist in *Opn4*$^{-/-}$ adults

An assessment of retinal vasculature in the *Opn4* mutant mice at P8 revealed promiscuous angiogenesis (Fig. 2). To determine whether melanopsin-dependent changes in retinal vascular pattern endured, we performed a quantitative assessment of retinal vascular development in *Opn4* mutant mice at P15, P25 and P180 (Fig. S3). At P15, all three plexi of the developing retina were significantly denser that normal (Fig. S3a, b, e). By P25, remodeling had returned the density of the superficial and deep vascular plexi to normal (Fig. S3f). By contrast, the middle layer remained significantly denser than normal (Fig. S3f) and this change was sustained until at least P180 (Fig. S3c, d, g). This indicated that the absence of melanopsin resulted in long-lasting increases in the density of the retinal vasculature but that after P15, this was regional and restricted to the middle vascular plexus.

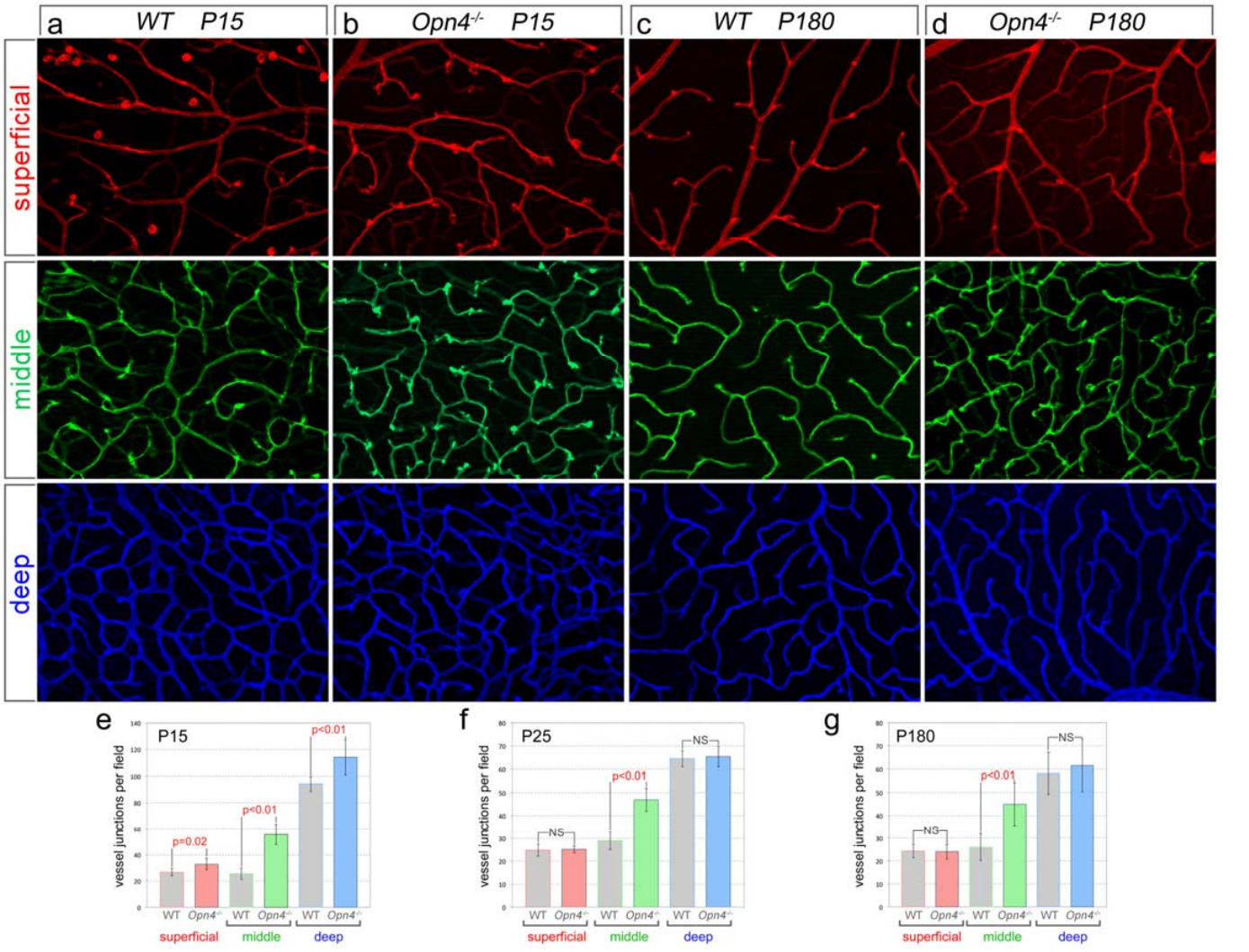

Figure S3 | Retinal vascular overgrowth is sustained until P180 in melanopsin mutant mice (a-d) Images of the superficial (red), middle (green), and deep (blue) vascular plexi in the retinae of P15 and P180 mice. (e, f, g) Quantification of vascular junctions at P15, P25 and P180 for the superficial (red), middle (green), and deep (blue) vascular plexi of wild type and *Opn4*$^{-/-}$ mice as labeled.

Figure S4. Hyaloid vessel development and regression is regulated by retinal Vegfa

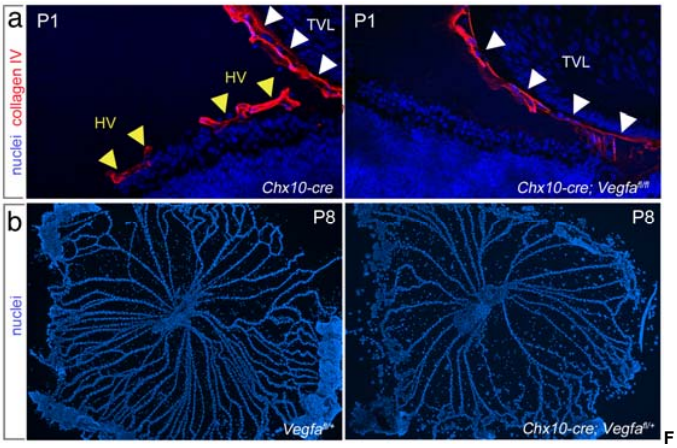

Figure S4 | Suppression of Vegfa expression in the retina is light and melanopsin-dependent. (a) Cryosections through the vitreous of control *Chx10-cre* and *Chx10-cre; VegfaA*$^{fl/fl}$ pups at P1 labelled for nuclei (blue) and collagen IV to identify blood vessels. White arrowheads indicate vessels of the tunica vasculosa lentis (TVL). Yellow arrowheads indicate hyaloid vessels (HV) present only in the control. (b) P8 hyaloid vessel preparations in control *Vegfa*$^{fl/+}$ and *Chx10-cre; Vegfa*$^{fl/fl}$ mice.

Deletion of a *Vegfa*^{fl} conditional allele from the lens results in a failure of development of the tunica vasculosa lentis (the capillaries adhered to the lens capsule) but has no effect on development of the hyaloid vessels adjacent to the retina[8]. This indicates that Vegfa has a local action. When the *Chx10-cre* retinal driver[9] was used to delete *Vegfa*^{fl}, the hyaloid vessels apparent in control mice (Fig. S4a, yellow arrowheads) failed to develop (Fig. S4a, right panel). The tunica vasculosa lentis was unaffected (Fig. S4a, white arrowheads). This showed that the hyaloid vessels were dependent on local retinal Vegfa for their formation but did not necessarily implicate Vegfa in hyaloid regression.

As an alternative, we performed heterozygous, *Chx10-cre* mediated *Vegfa*^{fl} deletion. We noticed that the control, *Vegfa*$^{fl/+}$ genotype consistently produced hyaloid vessel structures that were denser than normal at P8 (for example, compare Fig. 3b P8 control with Fig. 1a, P8 LD control). Though we do not have a detailed explanation for this, we cannot attribute this to genetic background because the increased hyaloid density tracks only with the *Vegfa*$^{fl/+}$ genotype. It is more likely that the *Vegfa*^{fl} allele design produces a mild over-expression of Vegfa that has a consequence for the hyaloid vessels. Despite this complication, assessment of the number of hyaloid vessels over a P1 to P8 time-course was revealing. At P1, control, *Vegfa*$^{fl/+}$ hyaloids were denser than the *Chx10-cre; Vegfa*$^{fl/+}$ experimentals (59±5 versus 48±4 vessels) indicating a developmental role for Vegfa. Regardless, when time-course data were expressed as relative capillary number (Fig. 3a) it was clear that the experimental *Chx10-cre; Vegfa*$^{fl/+}$ animals showed accelerated regression. This argues that the hyaloid vessels are sensitive to diminished levels of Vegfa during the normal phase of regression.

Figure S5. *Opn4* mutation results in elevated levels of Vegfa transcript in retinal neurons that are overrepresented

To identify retinal cell types that showed melanopsin-dependent *Vegfa* expression, we employed cell surface markers and flow-cytometry to isolate different retinal cell populations and compared the relative levels of *Vegfa* mRNA by QPCR between control and *Opn4*$^{-/-}$ mice. A Thy1.1+ population of RGCs was compared with Thy1.1-, Vc1.1+ amacrine/horizontal cells and Thy1.1-, Vc1.1-, PDGFR+ astrocytes. The astrocyte population showed no significant difference in *Vegfa* mRNA, but both RGCs and amacrine cells showed an increase (Fig. S5a). To determine whether development of these cell types might be influenced by a melanopsin-dependent pathway, we quantified the number of cells positive for either Brn3b (an RGC marker, Fig. S5b, c) or for calretinin (an amacrine cell marker) in P5 *Opn4*$^{-/-}$ mice. This showed that there were modest increases in the number of both Brn3b+ RGCs (30%) and calretinin+ amacrine cells (39%)(Fig. S5d). These data show that melanopsin is required for the down-regulation of *Vegfa* mRNA in some classes of retinal neurons but that it is also required to suppress the numbers of those neurons. We conclude that the increase in retinal and vitreal Vegfa in dark-reared and *Opn4*$^{-/-}$ mice is the result of both increased numbers of producer cells and increased transcript level.

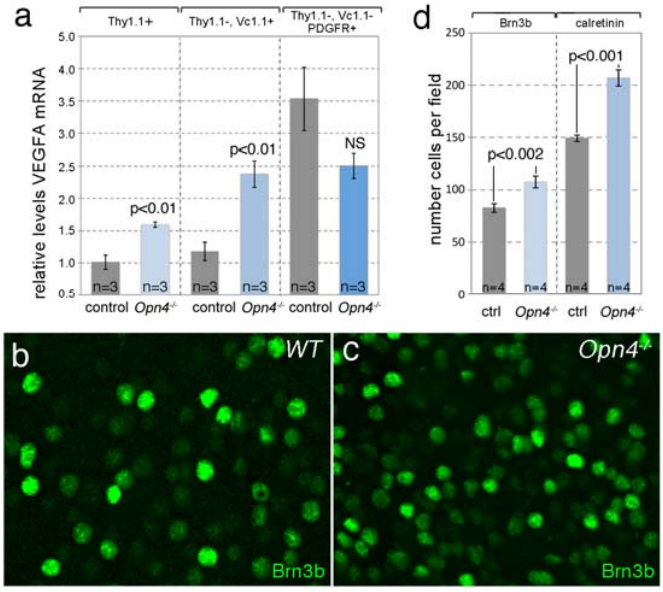

Figure S5 | Overrepresented retinal neurons express higher levels of Vegfa. (a) QPCR for *Vegfa* transcript in flow-sorted P5 retinal cell populations from control and *Opn4*$^{-/-}$ mice as labeled. (b, c) Labeling for the RGC marker Brn3b in wild type (b) and *Opn4*$^{-/-}$ (c) retina at P5. (d) Quantification of Brn3b and calretinin positive cells in whole-mount labeled retina of control and *Opn4*$^{-/-}$ mice at P5. For (a, d) p values determined by Student's T-test. NS – not significant. Errors bars are SEM.

Figure S6. Measurement of light levels in the visceral cavity of a mouse

Embryo transfer and enucleation experiments (Fig. 4) suggested that melanopsin in the fetus, not the mother, was critical to regulate neuronal and vascular development of the eye. This prompted us to assess whether visceral light levels might be sufficient to activate melanopsin expression ipRGCS according to published studies[10-12]. We first used a spectraradiometer to determine the light spectrum for mouse room fluorescent lights (Fig. S6a). We then calculated the portion of this spectrum that fell within the melanopsin spectral absorbance curve (Fig. S6b) and showed that the radiant flux density was 5.6 x 10^{13} photons/cm^2/sec. Equivalent measurements for sunlight (Fig. S6c, d) produced a melanopsin stimulating, radiant flux density of 2.6 x10^{16} photons/cm^2/sec. To estimate light attenuation across the mouse body wall, we directed a blue LED (peak wavelength=470 nm) positioned 1 inch from a miniature silicon photodiode detector either directly exposed or placed inside the abdominal cavity. The measurements were done on prone, live, anesthetized adult mice with the detector facing dorsally. Light attenuation was determined to be 0.6 (4 fold) and 1.7 (50 fold) log units in Balb/c and C57Bl6 mice, respectively. This meant that sunlight produced a visceral cavity flux density of 6.5 x 10^{15} (Balb/c) and 5.2 x 10^{14} (C57Bl6) photons/cm^2/sec while fluorescent lights gave 1.4 x 10^{13} (Balb/c) and 1.1 x 10^{12} (C57Bl6) photons/cm^2/sec. Placement of a blue LED in the visceral cavity of an anaesthetized mouse is a direct demonstration of light transmission across the body wall (Fig. 6e, f). Published response thresholds for rodent ipRGCs range upwards from approximately 1.2 x 10^{10} photons/cm^2/sec[10-12]. Though it has been suggested that ipRGCs in newborn mouse pups are less sensitive than in adults[11], the reduced sensitivity is about 1.5 log quanta and so the visceral light level in a pigmented animal of 1.1 x 10^{12} photons/cm^2/sec may still be above the threshold. These data are consistent with previous measurements[13] and with the hypothesis that the mouse fetus can respond directly to light via melanopsin.

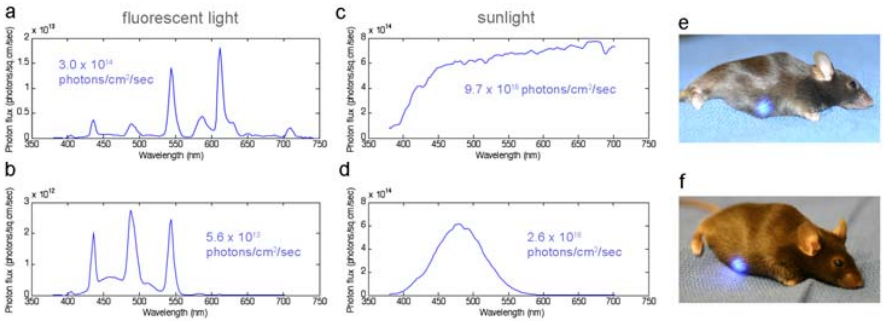

Figure S6 | Gestational light controls vascular development in the eye

(a-d) Spectrum and photon flux quantification for (a) fluorescent lights in the mouse room, (b) the portion of the spectrum in (a) capable of stimulating melanopsin, (c) sunlight, and (d) the portion of the spectrum in (f) capable of stimulating melanopsin. (h) Blue light LED within the visceral cavity of an anaesthetized mouse.

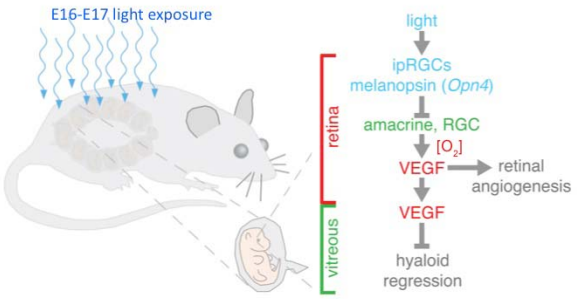

Figure S7 | Schematic describing the light response pathway that regulates retina development and vascularity. Based on the data presented, we suggested that melanopsin expressed in the fetus mediates a light response in the retina that regulates neuron number, oxygen demand, production of Vegfa and ultimately, postnatal vascular development.

References for Supplementary Information

1 Stefater, J. A., 3rd *et al.* Regulation of angiogenesis by a non-canonical Wnt-Flt1 pathway in myeloid cells. *Nature* **474**, 511-515, doi:10.1038/nature10085 nature10085 [pii] (2011).

2 Tarttelin, E. E. *et al.* Expression of opsin genes early in ocular development of humans and mice. *Exp Eye Res* **76**, 393-396, doi:S0014483502003007 [pii] (2003).

3 Graham, D. Melanopsin Ganglion Cells: A Bit of Fly in the Mammalian Eye. doi:NBK27326 [bookaccession] (1995).

4 Fu, Y., Liao, H. W., Do, M. T. & Yau, K. W. Non-image-forming ocular photoreception in vertebrates. *Curr Opin Neurobiol* **15**, 415-422, doi:S0959-4388(05)00104-2 [pii] 10.1016/j.conb.2005.06.011 (2005).

5 Ecker, J. L. *et al.* Melanopsin-expressing retinal ganglion-cell photoreceptors: cellular diversity and role in pattern vision. *Neuron* **67**, 49-60, doi:S0896-6273(10)00419-8 [pii] 10.1016/j.neuron.2010.05.023 (2010).

6 Hattar, S., Liao, H. W., Takao, M., Berson, D. M. & Yau, K. W. Melanopsin-containing retinal ganglion cells: architecture, projections, and intrinsic photosensitivity. *Science* **295**, 1065-1070, doi:10.1126/science.1069609 295/5557/1065 [pii] (2002).

7 Panda, S. *et al.* Melanopsin (Opn4) requirement for normal light-induced circadian phase shifting. *Science* **298**, 2213-2216, doi:10.1126/science.1076848 298/5601/2213 [pii] (2002).

8 Garcia, C. M. *et al.* The function of VEGF-A in lens development: formation of the hyaloid capillary network and protection against transient nuclear cataracts. *Exp Eye Res* **88**, 270-276, doi:S0014-4835(08)00257-1 [pii] 10.1016/j.exer.2008.07.017 (2009).

9 Rowan, S. & Cepko, C. L. Genetic analysis of the homeodomain transcription factor Chx10 in the retina using a novel multifunctional BAC transgenic mouse reporter. *Dev Biol* **271**, 388-402 (2004).

10 Sekaran, S. *et al.* Melanopsin-dependent photoreception provides earliest light detection in the mammalian retina. *Curr Biol* **15**, 1099-1107, doi:S0960-9822(05)00568-3 [pii] 10.1016/j.cub.2005.05.053 (2005).

11 Tu, D. C. *et al.* Physiologic diversity and development of intrinsically photosensitive retinal ganglion cells. *Neuron* **48**, 987-999, doi:S0896-6273(05)00891-3 [pii] 10.1016/j.neuron.2005.09.031 (2005).

12 Wong, K. Y. A retinal ganglion cell that can signal irradiance continuously for 10 hours. *J Neurosci* **32**, 11478-11485, doi:10.1523/JNEUROSCI.1423-12.2012 (2012).

13 Jacques, S. L., Weaver, D. R. & Reppert, S. M. Penetration of light into the uterus of pregnant animals. *Photochem Photobiol* **45**, 637-641 (1987).